A R C H I V E O F M E C H A N I C A L E N G I N E E R I N G

VOL. LXV 2018 Number 3

DOI: 10.24425/124486

Key words: Suter characteristics, pumping systems, centrifugal pump, power plant breakdown, transient analysis

KRZYSZTOF KARAŚKIEWICZ[1]

SENSITIVITY ANALYSIS FOR POWER PLANT PUMPING SYSTEMS IN BREAKDOWN

The small number of available complete modern pump characteristics makes the safety analysis of nuclear and conventional power plants based on the characteristics made over half a century ago of specific speeds n_q = 24.6, 147.1 and 261.4. The aim of the paper is to check sensitivity of the power plant system response for different complete pump characteristics – modern and available from older tests for n_q = 24.6, 147.1 and 261.4. It has been shown that Suter's characteristics for modern pumps give a different response to the pumping system of a power plant in breakdown than those used so far.

Nomenclature

List of basic symbols

h	dimensionless head $h = H/H_n$
q	dimensionless flow rate $q = Q/Q_n$
m	dimensionless torque $m = M/M_n$
α	dimensionless rotational speed $\alpha = n/n_n$
WH	Suter's head coefficient
WB	Suter's torque coefficient
X	Suter's flow/speed coefficient
n_q	specific speed $n_q = \dfrac{n\sqrt{Q}}{(H/stage)^{0.75}}$
δ_{WH}	relative uncertainty of extrapolated WH $\delta_{WH} = \Delta WH/WH$
δ_{WM}	relative uncertainty of extrapolated WM $\delta_{WM} = \Delta WM/WM$

Subscripts

n	nominal value

[1] *Institute of Heat Engineering, Warsaw University of Technology, Nowowiejska 21/25, 00-665 Warsaw, Poland. Email: krzysztof.karaskiewicz@itc.pw.edu.pl*

1. Introduction

In coal-fired stations, nuclear power stations and industrial power plants operate many pumps including feed water, condensate, cooling water pumps and secondary pumps.

During power failure, start-up or other unusual state the pumps can operate outside the normal area of operation [1–9].

Availability of such characteristic is very low. Mostly they come from non-industry tests. Pump manufactures deliver only basic characteristics ($Q > 0, H > 0$, $M > 0, n > 0$).

In [10] Suter characteristics were published for three specific speeds $n_q = 24.6$, 147.1 and 261.4. They are used for transient analysis by industry codes eg. RELAP Code. If pumps with other specific speeds are analyzed, such codes use extrapolated or interpolated values based on these three basic specific speeds.

Two kinds of uncertainty can be identified for characteristics so obtained. Firstly, they are based on the tests of pumps designed half a century ago, secondly due to the use of interpolation or extrapolation.

The 15Z33x8 feed water pump power failure was analyzed to check the influence of the characteristics uncertainty. The pump operated in typical pumping system between feed water tank and boiler for 200 MW unit.

Two kinds of Suter characteristics of modern pumps were used from [11] and [12]. They were compared to characteristic extrapolated from $n_q = 24.6$, 147.1 [10].

It was assumed that initial pumping system parameters change because of feed water control valve and motor power supply failures and pressure in feed water tank and boiler are constant.

2. Experimental characteristics

In the study [11] complete pump characteristics were measured for single stage pump of specific speed $n_q = 16$. The results were compared with measurements [12] for specific speed $n_q = 20$. Characteristics were represented in Suter form:

$$\begin{aligned} WH(X) &= \frac{h}{\alpha^2 + q^2}, \\ WM(X) &= \frac{m}{\alpha^2 + q^2}, \end{aligned} \tag{1}$$

where:

$$X = i\,\pi + \arctan\frac{q}{\alpha}, \qquad i = \begin{cases} 0 & \text{for } 0 \leqslant X \leqslant \dfrac{\pi}{2} \\ 1 & \text{for } \dfrac{\pi}{2} < X \leqslant \dfrac{3\pi}{2} \\ 2 & \text{for } \dfrac{3\pi}{2} < X \leqslant 2\pi \end{cases} \tag{2}$$

$$h = \frac{H}{H_n}, \qquad q = \frac{Q}{Q_n}, \qquad m = \frac{M}{M_n}, \qquad \alpha = \frac{\omega}{\omega_n}.$$

Fig. 1 shows the measured values of *WH(X)* and *WM(X)* for $n_q = 16$ and 20 in the whole range of $X \in \langle 0,\ 2\pi \rangle$.

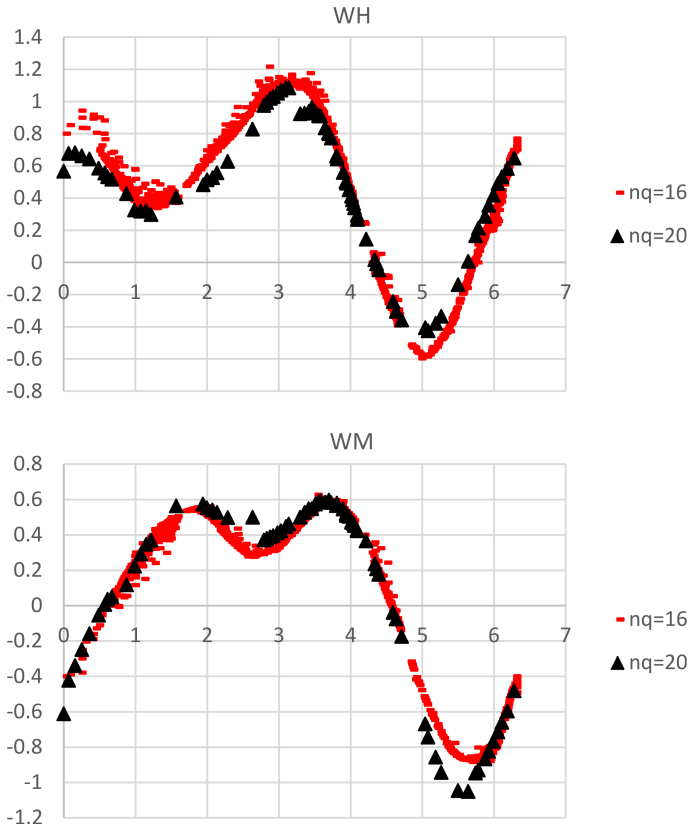

Fig. 1. *WH* and *WM* experimental data for specific speeds $n_q = 16$ and 20

The specific speeds are close to each other so one could expect *WH* and *WM* characteristics to be also close. There are some differences however for *WH* in the range of

- $0 < X <\sim 0.5$ dissipation zone – pump is driven in opposite direction, high static head makes negative flow – the case absent in the scope of the presented simulation;
- $\pi/2 < X < \pi$ dissipation zone – positive rotational speed and torque of pump with the negative flow;
- $3\pi/2 < X <\sim (9/5)\pi$ dissipation zone – pump is driven in opposite direction with negative head – the case absent in the scope of the presented simulation.

Some differences for *WM* mainly occur in dissipation zone $5 < X < 5.5$ for negative rotational speed and head but that zone is absent in the simulation.

3. Feed water system

The feed water system shown schematically in Fig. 2 is the feed pump 15Z33x8 that pumps water from the tank 1 through the heater 4 to the boiler 5.

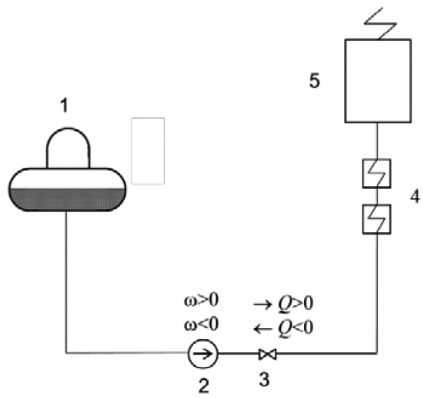

Fig. 2. Feed water pumping system: 1 – feed water tank, 2 – feed water pump, 3 – check valve, 4 – feed water heaters, 5 – boiler

Parameters of the pump set:

- rated flow $Q_n = 400$ m^3/h $= 0.111$ m^3/s,
- rated head $H_n = 2040$ m,
- rated head per stage $H = 256.25$ m,
- rated rotational speed $n_n = 3920$ rpm $\rightarrow \omega_n = 410.5$ rad/s,
- rated torque $M_n = 6333$ Nm,
- motor rated power $P_s = 3150$ kW,
- motor rated torque $M_n = 7674$ Nm,
- moment of inertia of rotating masses $I = 25.5$ kgm^2,
- specific speed resulting from the pump manufacturer's test $n_q = 19.5$.

Characteristics of the pumping system adopted on the basis of data for PKN Orlen:

$$H_{sys} = H_{stat} + aQ^2, \tag{3}$$

where: $H_{stat} = 1810$ m, $a = 18630$ s^2/m^5 for Q in m^3/s.

The length of the pipeline from the feed pump to the boiler is $l_1 = 70$ m and the pipeline diameter is $D_1 = 250$ mm. The length of the pipeline from the water tank to the pump is $l_2 = 40$ m and the pipeline diameter is $D_2 = 300$ mm.

Total length of the pipeline $l = l_1 + l_2 = 110$ m.

Equivalent diameter of the pipeline $D_n = \sqrt{\dfrac{4A_n}{\pi}} = 269$ mm, where

$$A_n = \frac{A_1 l_1 + A_2 l_2}{l_1 + l_2} = 5.694 \cdot 10^{-2} \text{ m}^2.$$

4. Basic equations and numerical model

The parameters of the pump operation during the breakdown are described by the equations

$$H(Q,\omega) = H_{stat} + aQ|Q| + \frac{l}{gA}\frac{\mathrm{d}Q}{\mathrm{d}t}, \tag{4}$$

$$M_s(Q,\omega) = I\frac{\mathrm{d}\omega}{\mathrm{d}t} + M_t + M_p, \tag{5}$$

where: M_s – motor torque, M_t – the sum of the friction moments in the gland and the bearings of the pump and motor, M_p – the moment passing to the liquid through the impeller of the pump (hydraulic torque).

The work of this moment is used to overcome the flow resistances of the pipeline and the inertia of the accelerated liquid mass $m = \rho l A_n$, where the liquid acceleration $a = \dfrac{\mathrm{d}c}{\mathrm{d}t} = \dfrac{1}{A}\dfrac{\mathrm{d}Q}{\mathrm{d}t}$.

Initial conditions for the pump are set down by its nominal parameters: $Q(0) = Q_n$, $\omega(0) = \omega_n$, $H(0) = H_n$ and $M_p(0) = M_n$, and for the motor by: $M_s = 0$.

For calculating the breakdown *WH(X)* and *WM(X)* characteristics are required (Fig. 3) in three zones:

- D (the first quadrant) for $\pi \leqslant X \leqslant\sim 1.38\pi$ (so-called normal operating area of the pump $H > 0$, $Q \geqslant 0$, $n \geqslant 0$, $M > 0$),
- C for $0.5\pi \leqslant X < \pi$, where, due to the predominance of the gravity of the water column above the force transmitted by the impeller ($\omega > 0$), backflow appears ($H > 0$, $Q < 0$, $n \geqslant 0$, $M > 0$),
- B for $\sim 0.6 \leqslant X < 0.5\pi$, where for $Q < 0$ the pump starts to rotate in the opposite direction ($H > 0$, $Q < 0$, $n < 0$, $M > 0$).

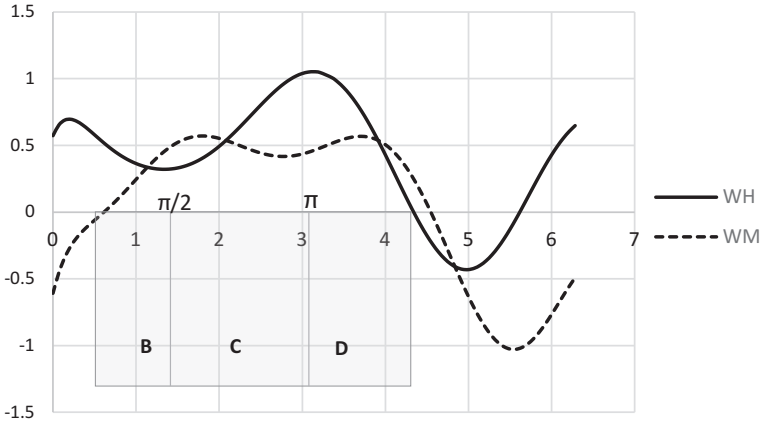

Fig. 3. Zones of pump operation after the power supply failure

In case of the first quadrant, the *WH* and *WM* could be achieved from flow characteristics for different speeds with torque calculated from

$$M = M_p = \frac{P}{\omega} = \frac{\rho g Q H}{\omega \eta} . \tag{6}$$

Usually such data is rarely available so one has to rely on the published characteristics of *WH* and *WM*.

5. Results of simulation of power supply failure

The simulation was performed for a relatively short time of about 1s to be assumed that the system parameters did not change.

The variable X being a function of the flow rate $Q(t)$ and the rotational speed $\omega(t)$ and therefore the function of time decreases from the value of $X = 5/4\pi$ to about 2.2. The range of X covered by the simulation was contained in zones D and C (Fig. 3).

The characteristics of the functions *WH(X)* and *WM(X)* for experimental and extrapolated data based on $n_q = 24.6$ and 147.1 according to [10] are shown in Figs. 4a and 4b.

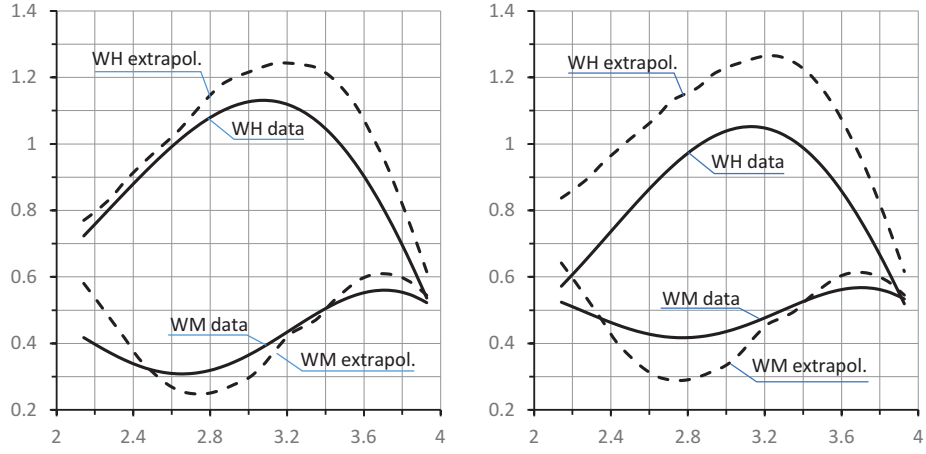

(a) $n_q = 16$ (b) $n_q = 20$

Fig. 4. Comparison of experimental and extrapolated *WH* and *WM* characteristics for $n_q = 16$ and 20 in the range of X

For both specific speeds in the range of X covered by the simulation, the *WH* and *WM* extrapolated characteristics differ largely from the experimental values.

Fig. 5 shows the relative uncertainties of *WH* and *WM* coefficients for extrapolated values based on Wylie and Streeter data [10].

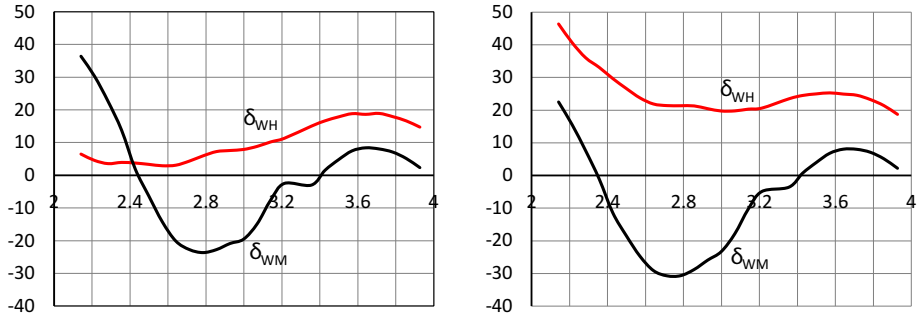

(a) $n_q = 16$ (b) $n_q = 20$

Fig. 5. Relative uncertainties δ_{WH} and δ_{WM} of extrapolated *WH* and *WM* characteristics for $n_q = 16$ and 20 in the X range covered by the simulation

The uncertainties are particularly large in the case of *WM* coefficient and exceed 30% locally.

The differences between extrapolated and measured data in turn, result in differences in the head $H(t)$ and torque $M(t)$, which affects the variations of the flow rate Q and speed ω.

Fig. 6 shows the heads for both specific speeds.

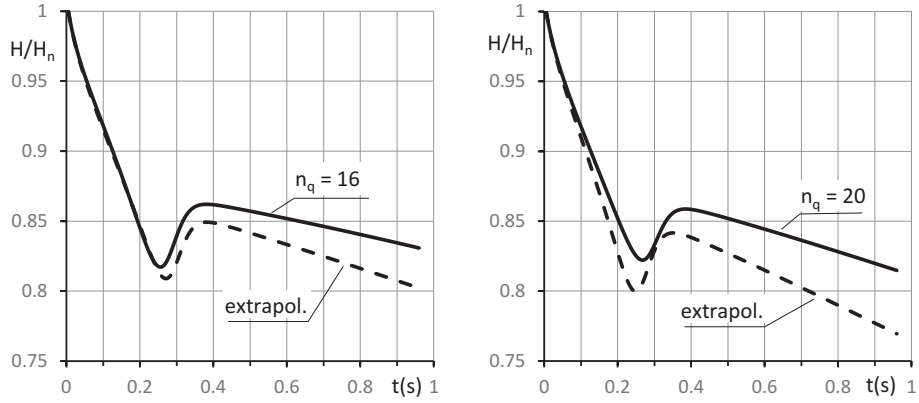

(a) $n_q = 16$ (b) $n_q = 20$

Fig. 6. H/H_n variations for $n_q = 16$ and 20

As a result of the change of flow direction, the head temporarily increases to start falling again under the influence of speed decreasing. There is a clear difference between the values of the extrapolated and experimental characteristics.

In the range $2 < X < 4$, both experimental curves *WH(X)* for $n_q = 16$ and 20 lie below the extrapolated curve based on Streeter data [10]. The lowest is the curve for $n_q = 20$. This affects the nature of $H(t)$ changes. The head falls the fastest for data $n_q = 20$ slightly slower for $n_q = 16$ and slowest for extrapolated values.

The local minimum occurs around 0.25 sec and is associated with passing through the maximum on the curve *WH(X)*.

Fig. 7 shows torque variation in the first second of breakdown.

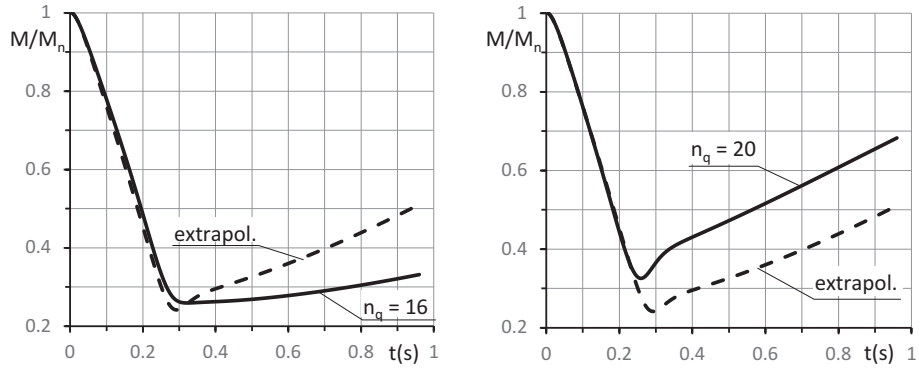

(a) $n_q = 16$ (b) $n_q = 20$

Fig. 7. M/M_n variations for $n_q = 16$ and 20

The torque initially drops but after the change of flow direction begins to rise and does not drop despite a decrease in rotational speed.

In both cases, differences in variations for experimental and extrapolated data are significant and increasing over time.

The average values of *WM* coefficients in the range of $2 < X < 4$ are $WM_{av} = 0.43$ for $n_q = 16$; $WM_{av} = 0.47$ for extrapolated and $WM_{av} = 0.49$ for $n_q = 20$. Consequently, at the end of the simulation, the largest value M is for $n_q = 20$ lower for extrapolated values and lowest for $n_q = 16$.

Figs. 8a and 8b show results of flow rate predictions after power failure.

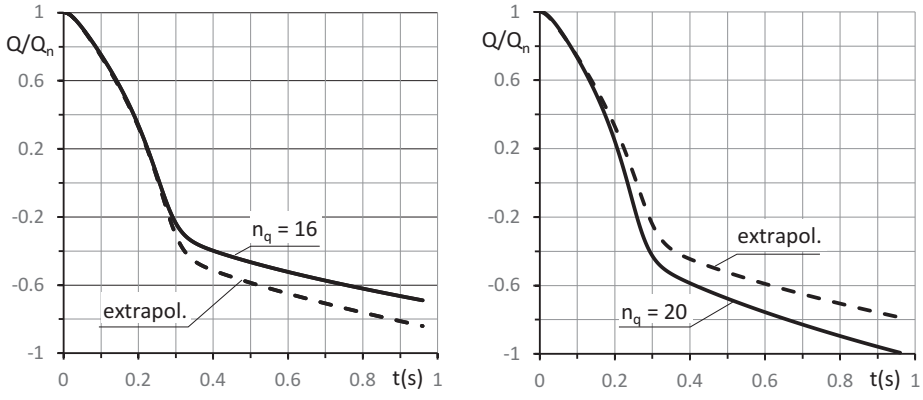

(a) $n_q = 16$ (b) $n_q = 20$

Fig. 8. Q/Q_n variations for $n_q = 16$ and 20

As a result of the drop in the pump head and the dominant influence of the system static head H_{st}, the flow begins to decrease and becomes negative.

The variation in flow is different for experimental and extrapolated specific speeds and that difference increases in time.

The deceleration of the flow depends on the difference between the force generated by the pump's impeller and the gravity force and the flow resistance and results from equation (4).

The slowest decreases the flow for $n_q = 16$ where the forces difference is the smallest and the fastest for $n_q = 20$ where the forces difference is the largest one.

Figs. 9a and 9b show the variations in rotational speed during a failure.

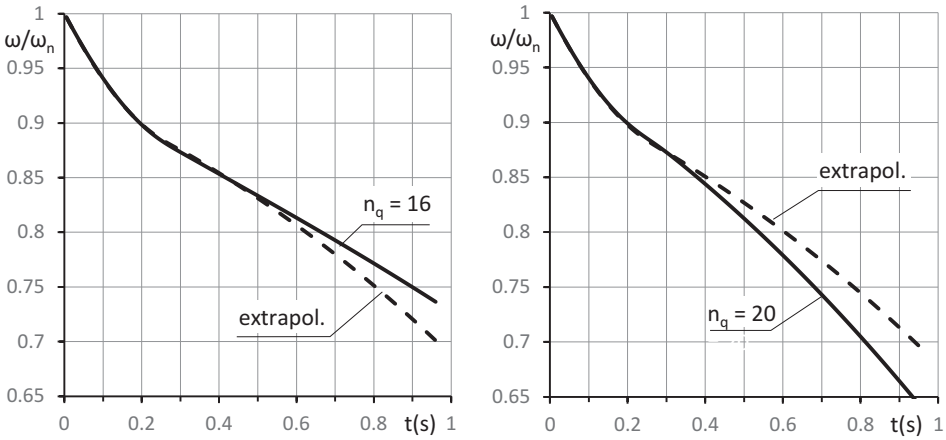

(a) $n_q = 16$ (b) $n_q = 20$

Fig. 9. ω/ω_n variations for $n_q = 16$ and 20

Extrapolated and experimental predictions disperse over time. In this case, it is more significant for $n_q = 20$.

The higher the pump torque which is associated with the higher *WM* coefficient the faster slowing down of the flow rate in the system, according to the equation (5). The final rotational speeds are correlated with the pump torques. The highest moment and therefore the lowest final speed is for the case $n_q = 20$ and the lowest final torque and the highest final rotational velocity for the case $n_q = 16$.

Breakdown simulation is performed in the X range in which there are clear differences between the extrapolated and experimental values. These differences clearly affect the results of the simulation, which shows that new research on modern pumps for different specific speeds is needed. Applying the values published in [10] based on the tests of non-produced pumps can lead to errors that change the picture of the brakedown.

6. Summary

The work compares the complete characteristics of contemporary pumps obtained from the tests for specific speeds $n_q = 16$ and 20 most similar to the specific speed of the 15Z33x8 pump.

In the area covered by the simulation, the pump characteristics for specific speeds $n_q = 16$ and 20 differ. They are also different from the characteristics obtained by extrapolation based on Streeter data.

In order to verify the sensitivity of the system to the differences in the complete characteristics of modern pumps and pumps produced half a century ago, a simulation of breakdown in power plant feed water system was carried out by motor power supply failure and the check valve failure.

Simulation shows a clear difference between the results obtained from extrapolation based on Streeter data, used in some commercial codes (e.g. RELAP), and the results based on the current study of the modern pumps.

The impact of the extrapolation error was not taken into account in the analysis due to the lack of appropriate accurate data.

This study shows that with relatively small differences in the specific speeds, there may be distinct differences in the corresponding Suter characteristics. These differences may be partly due to the lack of similarity in the pump parts other than the impeller (e.g. volute, suction nozzle).

The pump characteristics obtained by extrapolating Streeter data generates a different dynamics of pump parameters than in case of the characteristics of modern pumps. The sensitivity of the system to the characteristics is quite large, which encourages the use of the most accurate data possible to improve the accuracy of the simulation of the pumping systems in transient state.

Manuscript received by Editorial Board, March 14, 2018;
final version, June 15, 2018.

References

[1] W. Jędral, K. Karaśkiewicz, and J. Szymczyk. Study of the complete characteristics of centrifugal pumps. *Scientific Works of Warsaw University of Technology. Conferences*, 27:79–87, 2011 (in Polish).

[2] W. Jędral, K. Karaśkiewicz, and J. Szymczyk. Unsteady states of operation and complete characteristics of centrifugal pumps. *Pompy, Pompownie*, 1(148):41–44, 2013 (in Polish).

[3] W. Jędral, K. Karaśkiewicz, and J. Szymczyk. Studies of transients and complete characteristics of centrifugal pumps. *Instal*, (11):21–24, 2013 (in Polish).

[4] W. Jędral, K. Karaśkiewicz, and J. Szymczyk. Pump transients and complete pump performance characteristics. *Journal of Power Technologies*, 94(3):196–201, 2014.

[5] W. Jędral, K. Karaśkiewicz, and J. Szymczyk. The complete characteristics of centrifugal pumps and the method of their approximate determination. *Pompy, Pompownie*, 2(149):28–31 2013 (in Polish).

[6] Y. Lahssuny. *Transients caused by the pump coastdown in pressurized water reactors*. Ph.D. Thesis, Warsaw University of Technology, 1996.

[7] W. Jędral and K. Karaśkiewicz. Start-up of axial-flow pump at initial reverse flow. *Pompy, Pompownie*, 107(4):30–34, 2002 (in Polish).

[8] R. Zhu, Y. Liu, X. Wang, Q. Fu, A. Yang, and Y. Long. The research on AP1000 nuclear main pumps' complete characteristics and the normalization method. *Annals of Nuclear Energy*, 99:1–8, 2017. doi: 10.1016/j.anucene.2016.08.014.

[9] I.A. Lipatov, I.V. Elkin, A.I. Antonova, G.I. Dremin, A.V. Kapustin, S.M. Nikonov, A.A. Rovnov, and V.I. Gudkov. Four-quadrant characteristics of PSB-VVER pumps. Proceedings of the International Conference "Nuclear Energy for New Europe 2005", pages 056.1–10, Bled, Slovenia, September 5–8, 2005.

[10] E.B. Wylie and V.L. Streeter. *Fluid Transients in Systems*, Prentice Hall, Englewood Cliffs, 1993.

[11] W. Jędral. Research and application of complete centrifugal pump characteristics to increase their reliability and energy efficiency in liquid transport, especially in power engineering. Research project nr NN513 331038 (grant MNiSW), Warsaw, 2010 (in Polish).

[12] E. Ayder, A.N. Ilikan, M. Şen, C. Özgür, L. Kavurmacıoğlu, and K. Kirkkopru. Experimental investigation of the complete characteristics of rotodynamic pumps. ASME 2009 Fluids Engineering Division Summer Meeting, pages 35-40, Vail, Colorado, 2-6 August, 2009. doi: 10.1115/FEDSM2009-78052.